Equivalent Circuit Synthesis of Plant Cell Vacuole by Fitting on 2-3 GHz Resonant Frequencies

Koyu Chinen[1*], Ichiko Kinjo[2]
[1]GLEX, Japan,
Email: koyu.chinen@nifty.com,
[2]National Institute of Technology, Okinawa College, Japan,
Email: ichi@okinawa-ct.ac.jp
[*] *Corresponding author*

Abstract: **The reflective S-parameters S11 of pure water and five plants of pear, tomato, carrot, ginger, and potato, representing fruits, vegetables, and root vegetables, were measured using a highly sensitive five-pin SMA probe, five times higher than an open-end SMA probe, and the admittance curves were plotted on a Smith chart. The cell vacuole was extracted by grinding and filtering through a 20-micron filter. A specific circle feature and resonant frequencies were observed at high frequencies above 2 GHz in the admittance curve over a frequency range of 1 to 4000 MHz. Equivalent circuits were synthesized using curve fitting on strict values of serial and parallel resonant frequencies when the susceptance, j*B*, equals zero, and the circuit element values of *C*, *R*, and *L* were determined. The values of the elements were related to the polar molecule H_2O, K ions, and SMA probe configuration. The simulated and calculated values of admittance, circuit elements, and resonant frequencies, determined using synthesized equivalent circuits and derived equations, are consistent with the measured values. Since the cell vacuole substantially consists of polar molecule H_2O and K ion, and the NaCl solution consists of H_2O and Na and Cl ions, the strict value of the NaCl solution can be used as a reference for the admittance value of the cell vacuole.**

Keywords: **Plant cell vacuole, Fruit and vegetable, Plant equivalent circuit, EIS, S-parameter, Resonant frequency**

I. INTRODUCTION

The plant cells of vegetables and fruits are primarily composed of the cell wall and the cell vacuole. The investigation of the electrical characterization of these parts contributes to clarifying the agricultural and biological properties of the plants [1]. Electrical impedance spectroscopy (EIS) has been used to investigate the electrical mechanism of biological and chemical materials [2–4]. The EIS method was used to measure the impedance and synthesize the electrical equivalent circuits of food [5], plants [6–8], NaCl solutions [9, 10], and alcohols [11, 12]. This technology has been utilized to enhance agricultural productivity, develop new species, and prevent disease.

The EIS method generally limits the measurement frequency to a low-frequency range due to the use of an I-V instrument, such as an impedance analyzer. On the other hand, the authors have used an S-parameter measurement method using a network analyzer. This technology enables the authors to measure the impedance of aqueous solutions [13] in a high-frequency range, alcohols [14], plants [15], cell walls [16], and cell vacuoles [17], and to synthesize equivalent circuits for these systems.

In this study, the authors evaluated the scattering (S) parameters measured for plant samples of fruits and vegetables over a high-frequency range using a specially designed subminiature version A (SMA) probe to increase the measurement sensitivity. So far, an open-ended SMA probe has been used in measurements within a high-frequency range, although it has a low sensitivity. The authors designed, for the first time, a highly sensitive multi-pin SMA probe. The multi-pin SMA probe exhibits a specific feature in the plotted S-parameter curve. The authors have developed, for the first time, an accurate method for synthesizing the equivalent circuit of the plant cell vacuole utilizing a particular resonant frequency technique. The conventional curve fitting used to synthesize the equivalent circuit has an accuracy problem that depends on human skill.

II. S-PARAMETER AND ADMITTANCE MEASUREMENTS FOR PLANT SAMPLES

The authors prepared pure water and five plants: pear, tomato, carrot, ginger, and potato to measure the scattering parameter (S-parameter) in the frequency range of 1 MHz to 4000 MHz. The measured sample number of each plant was more than four. Two vector network analyzers (VNAs), the LiteVNA and the PNA-L VNA (N5230A) [18], were used to confirm the accuracy and ensure reproducibility when measuring the reflection coefficient S_{11}. A highly sensitive five-pin SMA probe consists of a central signal pin (gold-plated copper, 4 mm × 0.8 mm-diameter) surrounded by polytetrafluoroethylene (PTFE) and four ground pins (4 mm apart from the signal pin). The VNA and SMA-probe instruments were calibrated using an SMA standard set of short, open, load, and through (SOLT). The measurement accuracy was confirmed using a surface-mount device (SMD) resistor soldered on the five-pin SMA. The SMA probe was inserted into the plant sample during measurement of the S-parameters. When the authors use LiteVNA, the application software of Nanovna-saver [19] was used to convert the measured voltage to the S-parameter. The reflection coefficient S_{11} of the S-parameter is the ratio of the reflected voltage $V_r = A\varepsilon^{\gamma x}$ to the forward voltage $V_f = B\varepsilon^{-\gamma x}$, expressed as $S_{11} = V_r / V_f$. The admittance Y is calculated using the S_{11} and expressed as $Y = (1\text{-}S_{11}) / (1\text{-}S_{11})$. Complex numbers, including amplitude and phase information, express these values.

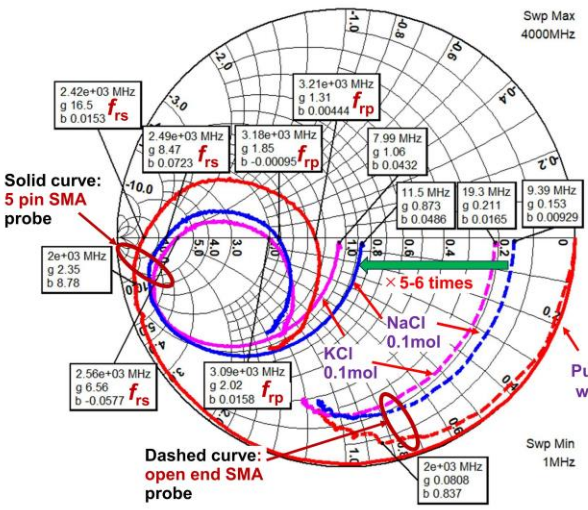

Fig. 1. The reflective S-parameter values, S_{11}, were measured for pure water, NaCl, and KCl solutions using an open-end SMA probe and a five-pin SMA probe, at frequencies from 1 MHz to 4 GHz.

Figure 1 shows the measured and plotted S_{11} reflective S-parameters for pure water, a 0.1 mol/L NaCl solution, and a 0.1 mol/L KCl solution, using both an open-end SMA probe and a five-pin SMA probe, at frequencies ranging from 1 MHz to 4 GHz. The sensitivity, determined by the conductance value (G), of the five-pin SMA probe, is 5 to 6 times higher than that of the open-end SMA probe. The open-end measured approximately less than 2 GHz without fluctuation, whereas the five-pin SMA probe exhibited approximately 4 GHz with a clear and smooth plot curve; hence, a frequency range of measurement approximately two times wider for the susceptance jB is expected with the five-pin SMA probe. Furthermore, the five-pin SMA probe exhibits precise resonant frequencies that can be used to characterize the pure water, NaCl, and KCl solutions. The superiority of the five-pin SMA probe in terms of sensitivity is attributed to its high-capture design in the sample.

Figure 2 shows the measured reflection coefficient, S11, plotted on the impedance and admittance grids for water and five plants of pear, tomato, carrot, ginger, and potato. These plant samples represent fruits, vegetables, and root vegetables. The plotted data represent the average value of five samples of each plant. Each curve has a bending point between 7 and 25 MHz. The plotted curve, at frequencies lower than the bending point, is plotted along the impedance grid. The equivalent circuits can be synthesized using serial and parallel circuits for lower and higher frequencies, respectively, than the vending point.

A plant cell is composed of a cell wall, membrane, nucleus, and vacuole. The vacuole occupies 70-90% of the cell and contains polar molecules (H_2O) and ions of potassium (K^+), sodium (Na^+), calcium (Ca^{2+}), magnesium (Mg^{2+}), and phosphorus (P^-). The cell wall consists of cellulose, a highly electrically resistant and low-capacitance material. The S-parameter S_{11} values were measured before and after the 20-μm filtering, as shown in Fig. 3. Before filtering, the plotted S_{11} curve shows a cell wall. After the filtering, the plotted curve shows a high admittance and no bending point. A signal with a frequency lower than the frequency at the bending point is not transparent in the plant cell due to the cell wall. The equivalent circuit of the cell wall consists of a serial sub-circuit of resistance and capacitance. When the frequency is increased, the signal passes through the cell wall.

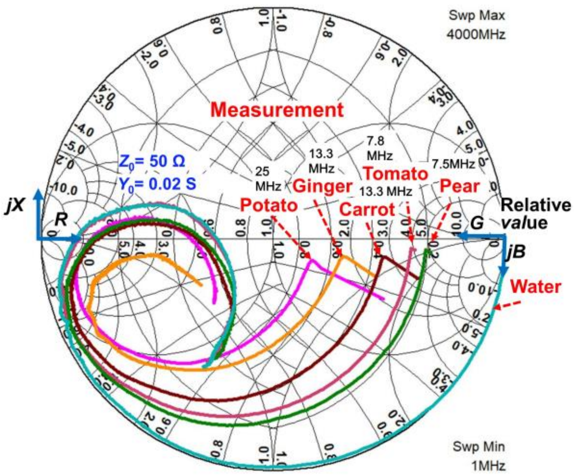

Fig. 2. The reflective S-parameter values, S_{11}, measured for six samples of pure water, pear, tomato, carrot, ginger, and potato, are plotted on impedance and admittance grids of a Smith chart.

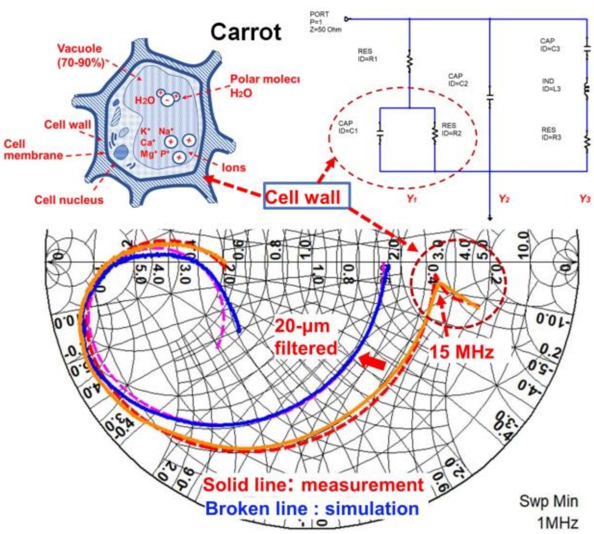

Fig. 3. A typical plant cell consists of a vacuole, a cell wall, a cell membrane, and a cell nucleus. The S-parameter S_{11} values were measured before and after the 20-μm filtering. Before filtering, the plotted S_{11} curve shows a cell wall part. After the filtering, the plotted curve shows a high admittance and no bending point. An equivalent circuit was synthesized using curve fitting, and S_{11} values simulated using the equivalent circuit are plotted with a broken line.

III. SYNTHESIS OF EQUIVALENT CIRCUIT OF PLANT CELL

Since most of the measured curve is plotted along the admittance grid, a parallel circuit can be considered as the equivalent circuit. Using curve fitting, an equivalent circuit is synthesized. The authors used two RF circuit simulators, QucsStudio [20] and AWR-MWO [21], for the curve fitting. The synthesized equivalent circuit consists of three sub-circuits: Y_1, Y_2, and Y_3.

Five plants, pear, tomato, carrot, ginger, and potato, were ground and filtered with a 20-µm filter, and the reflective S-parameters were measured and plotted on a Smith chart. The measurement setup, with the five-pin SMA probe, used for the cell vacuole shown in Fig. 4, is identical to that used for measuring five samples before the grating and filtering. It is noted that the measured bending point disappears after filtering in the plotted curves.

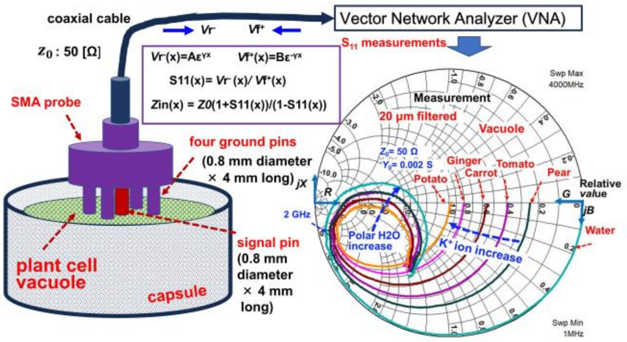

Fig. 4. After grinding and filtering with a 20-µm filter, the reflective S-parameter S_{11} values were measured using the setup, with the five-pin SMA probe, identical to that used for measuring samples before grinding and filtering, for the six samples of water, pear, tomato, carrot, ginger, and potato and plotted on the admittance grid of a Smith chart. The grinding and 20-µm filtering removed the cell wall part in the admittance curve.

The equivalent circuit of the vacuole, synthesized using curve fitting of the measured admittance curves, is shown in Fig. 5. The resistance R_1 primarily relates to the conductance due to K^+ ions at low frequency. The capacitance C_2 relates to the permittivity of the polar molecule (H_2O). The serial sub-circuit, consisting of capacitance C_3, inductance L_3, and resistance R_3, relates to the electrical interaction between the H_2O and the SMA electrode configuration.

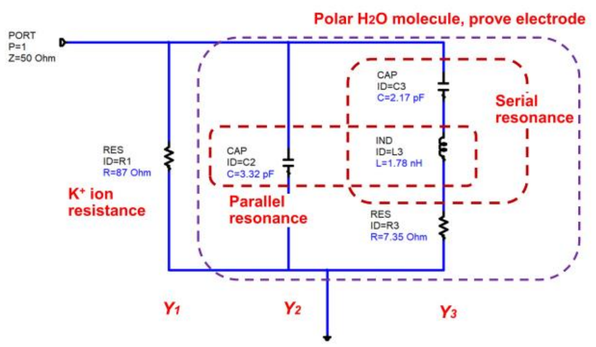

Fig. 5. An equivalent circuit was synthesized from the measured admittance data of Y, G, and jB. The resistance R_1 is related to the concentration of potassium K^+ ions. The capacitance C_2 relates to the permittivity of the polar H_2O. The C_3, L_3, and R_3 relate to the combination and interaction between polar H_2O and SMA configuration.

IV. EQUIVALENT CIRCUIT ELEMENT VALUES DERIVED BY RESONANT FREQUENCY

After grinding and filtering, the reflective S-parameters S_{11} and admittance were measured. The measured admittance (Y), conductance (G), and susceptance (jB) are plotted on the Cartesian coordinate, as shown in Fig. 6. The susceptance jB curve exhibits two resonant frequencies corresponding to serial and parallel resonance. The equivalent circuit element values are determined through curve fitting of the susceptance jB curve. Since the resonant frequencies are precise, the curve fitting accuracy using the susceptance jB curve is higher than that of the conventional admittance curve Y.

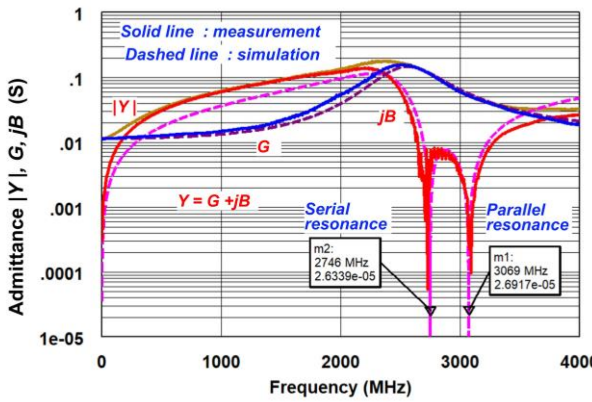

Fig. 6. The admittance $|Y|$, the conductance G, and the susceptance jB were measured from the reflective S-parameter and derived from the synthesized equivalent circuit of the cell vacuole. The solid and dashed lines show measured and simulated values, respectively. The jB curves exhibit the serial and parallel resonant frequencies.

The admittance Y of the synthesized equivalent circuits of the plant cell, as shown in Fig. 5, can be calculated using Kirchhoff's theory. The admittance Y is the sum of the sub-circuits: Y_1, consisting of R_1, C_1, and R_2; Y_2, consisting of C_2; and Y_3, consisting of C_3, L_3, and R_3.

$$
\begin{aligned}
Y &= Y_1 + Y_2 + Y_3 \\
&= \frac{R_2 - j\frac{1}{\omega C_1}}{R_1\left(R_2 - j\frac{1}{\omega C_1}\right) - j\frac{R_2}{\omega C_1}} + j\omega C_2 + \frac{1}{R_3 + j\omega L_3 - j\frac{1}{\omega C_3}} \\
&= \frac{R_1(\omega C_1 R_2)^2 + (R_1 + R_2)}{{R_1}^2(\omega C_1 R_1)^2 + (R_1 + R_2)^2} + \frac{R_3}{{R_3}^2 + (\omega L_3 - \frac{1}{\omega C_3})^2} \\
&\quad + j\left[\frac{\frac{1}{\omega C_1}(\omega C_1 R_2)^2}{{R_1}^2(\omega C_1 R_2)^2 + (R_1 + R_2)^2} + j\omega C_2 - \frac{(\omega L_3 - \frac{1}{\omega C_3})^2}{{R_3}^2 + (\omega L_3 - \frac{1}{\omega C_3})^2}\right]
\end{aligned} \tag{1}
$$

When the cell wall is removed by grinding and filtering, the resistance R_2 equals zero. In the case of resonance, the imaginary part (susceptance jB) equals zero.

$$\omega_r C_2 \left[{R_3}^2 + (\omega L_3 - \frac{1}{\omega C_3})^2 - (\omega L_3 - \frac{1}{\omega C_3}) \right] = 0 \tag{2}$$

The resonant angular frequency ω_r^2 is determined using the quadratic formula.

$$\omega_r{}^2 = \frac{1}{2{L_3}^2 C_2} K_2 \pm \sqrt{{K_2}^2 - {L_3}^2({K_1}^2 - 1)} \tag{3}$$

where, $K_1 = (2C_2) / C_3 + 1$ and $K_2 = L_3 K_1 - C_2 R_3^2$.

The resonant frequency is determined by $f_r = \omega_r / (2\pi)$.

According to (3) and the synthesized equivalent circuit, the resonant frequency (f_r) has two values, the serial and parallel frequencies. Although the algorithm determining the admittance Y expressed by (1) differs from that of the computer simulations, such as QucsStudio and AWR-MWO, because the computer simulation generally determines the circuit node voltage by solving a system of equations, where the sum of the single-frequency sinusoidal currents at the node of the circuit is zero, it was confirmed that the calculated admittance Y, as expressed in (1), is consistent with the result of the computer simulations.

Synthesized equivalent circuit element values of the vacuole for four plants of pear, tomato, carrot, and ginger are determined using curve-fitting on the resonant frequencies of jB and plotted on the Cartesian coordinate, as shown in Fig. 7. The synthesized equivalent circuit component values of R_1, C_2, C_3, L_3, and R_3 for the six samples of water, pear, tomato, carrot, ginger, and potato, and four different NaCl molar concentrations of 0.01, 0.025, 0.05, and 0.1 mol/L are derived from the resonant condition when the susceptance jB equals zero and plotted in Fig. 8. The equivalent circuit of the NaCl solution is the same as that of the cell vacuole. The inverse of the amount of potassium (K^+) per 100 g of the sample [22], K^+amt, is plotted and shows a similar curve to R_1.

The resistance R_1, consisting of the sub-circuit Y_1, relates to the conductance of ions in the vacuole. The majority of the ions are potassium (K^+) ions, accounting for approximately 70 - 90% in the five samples [22]. The capacitance C_2, consisting of the sub-circuit Y_2, relates to the permittivity of the polar molecule H_2O. The capacitance C_3, inductance L_3, and resistance R_3 are related to the combination and interaction of the H_2O and SMA-electrode. C_2 and L_3 determine the parallel frequency, and the serial frequency is determined by C_3, L_3, and R_3, as shown in (3). The measured and calculated parallel and serial frequencies are consistent, as shown in Table 1.

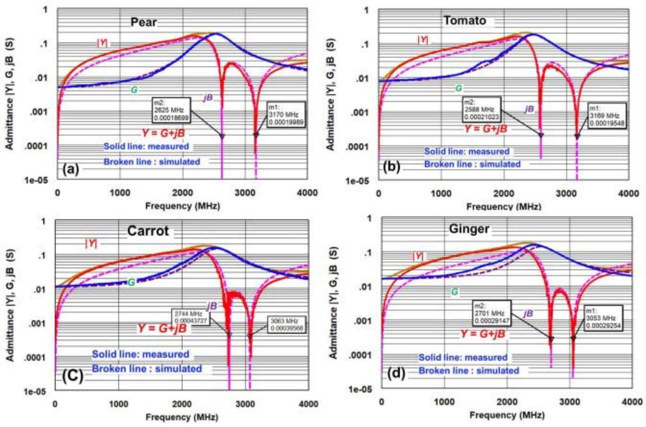

Fig. 7. The measured and simulated admittance $|Y_{11}|$, conductance G, and susceptance jB values for (a) pear, (b) tomato, (c) carrot, and (d) ginger.

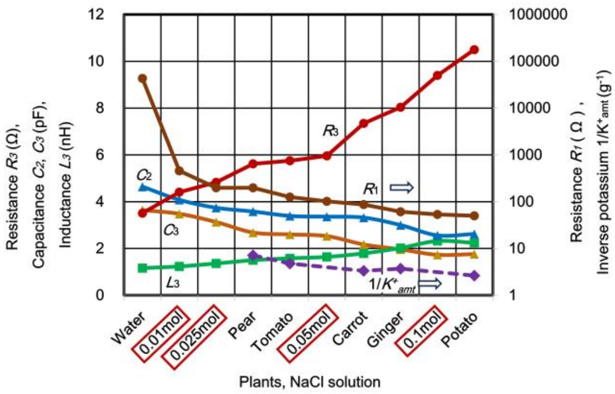

Fig. 8. The synthesized equivalent circuit component values of R_1, C_2, C_3, L_3, and R_3 for the six samples of water, pear, tomato, carrot, ginger, and potato, and four different NaCl molar concentrations of 0.01, 0.025, 0.05, and 0.1 mol/L are derived from the resonant condition when the susceptance jB equals zero. The equivalent circuit of the NaCl solution is the same as that of the cell vacuole. The inverse of the amount of potassium K^+ per 100 g of the sample [22], K^+_{amt}, is plotted and shows a similar curve to R_1.

TABLE I. EQUIVALENT CIRCUIT ELEMENT VALUES OF R_1, C_2, C_3, AND L_3, AND CALCULTAED AND MEASURED SERIAL AND PARALLEL RESONANT FREQUENCIES.

Sample	R_1	C_2	C_3	L_3	R_3	f_{rsc}	f_{rpc}	f_{rsm}	f_{rpm}
Water	43200	4.64	3.64	1.16	3.51	2.52	3.20	2.51	3.20
$NaCl_{0.01}$	458	4.08	3.48	1.23	4.41	2.52	3.19	2.53	3.19
$NaCl_{0.025}$	198	3.74	3.13	1.36	4.83	2.53	3.19	2.54	3.19
Pear	198	3.58	2.68	1.50	5.62	2.63	3.17	2.64	3.17
Tomato	126	3.39	2.60	1.58	5.75	2.59	3.17	2.59	3.16
$NaCl_{0.05}$	102	3.36	2.53	1.64	5.96	2.58	3.13	2.59	3.14
Carrot	87	3.32	2.17	1.79	7.35	2.74	3.06	2.75	3.07
Ginger	61	3.00	1.96	2.02	8.04	2.70	3.05	2.70	3.04
$NaCl_{0.1}$	53.5	2.56	1.73	2.32	9.40	2.68	3.05	2.68	3.08
Potato	50	3.11	2.0	1.94	9.76				
Unit	Ω	pF	pF	nH	Ω	GHz	GHz	GHz	GHz

V. EQUIVALENT CIRCUIT ELEMENTS OF VACUOLE AND NACL SOLUTION

The reflective S-parameters S_{11} were measured for four different NaCl molar concentrations of 0.01, 0.025, 0.05, and 0.1 mol/L and plotted on the admittance grid of a Smith chart, as shown in Fig. 9. The plotted curves show a similar feature of a circle curve above 2 GHz to the plant cell vacuole. Since the NaCl molar concentration is a strict standard value, the NaCl solutions can be used as a reference when evaluating the admittance of the plant cell vacuole. The admittance curves of the five sorts of plant cell vacuoles are between 0.01 and 0.1 mol/L NaCl solutions. Since the natural water and the human body have NaCl molar concentrations of approximately 0.001 and 0.154 mol/L, respectively, the admittance characteristics of six plant vacuoles are similar to those between the natural water and the human body.

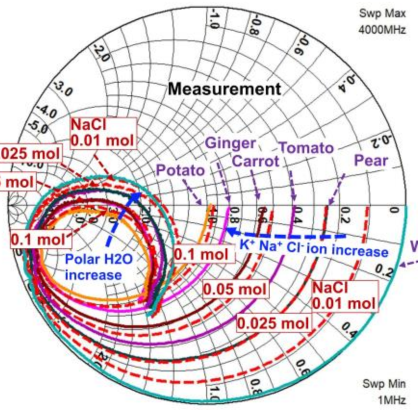

Fig. 9. After grinding and 20-µm filtering, the reflective S-parameter S_{11} values of the six samples of water, pear, tomato, carrot, ginger, and potato are plotted on the admittance grid of the Smith chart. For reference, the reflective S-parameter S_{11} values of NaCl solutions with four different molar concentrations of 0.01, 0.025, 0.05, and 0.1 mol/L are plotted on the admittance grid.

The NaCl solutions have the same equivalent circuit and an admittance characteristic as the plant cell vacuole. The equivalent circuit element values are determined by fitting to two resonant frequencies: one serial and one parallel frequency when the susceptance (jB) equals zero. The R_1 values are related to K^+ and Na^+ ions for plant cell vacuoles and NaCl solutions. The C_2 values are associated with the polar molecule H_2O. The C_3, L_3, and R_3 are related to the combination and interaction between H_2O, ions, and the SMA probe. The five-pin SMA probe exhibits high sensitivity when measuring the reflective S-parameter S11, and it has an inductance value of L_3. Therefore, it exhibits resonant frequencies at high frequencies above 2 GHz, but it enables the determination of the accurate equivalent circuit element values. The plant cell vacuole consists of polar molecules, including water (H_2O) and potassium (K^+) ions. Since the polar molecule H_2O responds to the high-frequency signal, it rotates and vibrates, thereby determining the component value of C_2. The potassium K^+ and hydrated ions react to low-frequency signals, thereby determining the component value of R_1. When the potassium K^+ concentration increases, the friction and collision between the polar molecule H_2O and ions thereby increases the resistance R_3 and inductance L_3.

The synthesized equivalent circuit components of R_1, C_2, C_3, L_3, and R_3 determined by fitting resonant frequencies on the susceptance jB curve for the plant cell vacuole and NaCl solution are listed in Table 1. The serial and parallel resonant frequencies, f_{rsc} and f_{rpc}, are calculated using (3) and the derived component values. The calculated and measured resonant frequencies, f_{rsc} and f_{rsm}, and f_{rpc} and f_{rpm}, respectively, are consistent, as shown in Fig. 10.

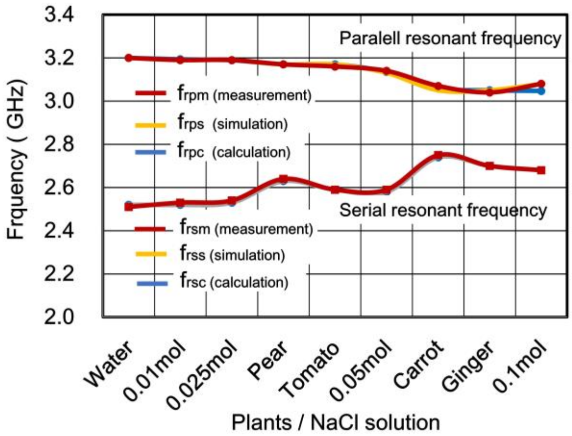

Fig. 10. The measured, simulated, and calculated parallel resonant frequencies (f_{rpm}, f_{rps}, and f_{rpc}) and serial resonant frequencies (f_{rsm}, f_{rss}, and f_{rsc}) for water, pear, tomato, carrot, ginger, and 0.05-0.1 mol/L NaCl solutions.

The sorts of ions of the plant cell vacuole are potassium (K^+), sodium (Na^+), and calcium (Ca^{2+}). magnesium (Mg^{2+}), and phosphorus (P^+). The potassium (K^+) ion content is a significant amount, exceeding 80 % for the five plants of pear, tomato, carrot, ginger, and potato. When plotting the inverse of the amount of K^+ (mg / 100g) [22], the curve of the $1/K^+$ shows the same feature as the R_1 value, as shown in Fig. 8. Hence, the R_1 value is determined by the potassium (K^+) ion.

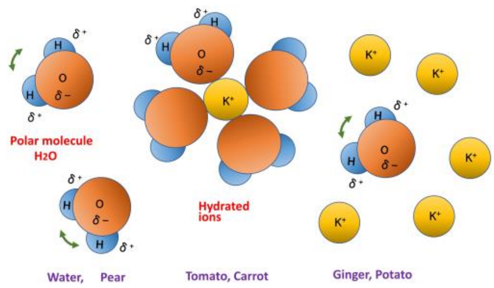

Fig. 11. The polar molecule H_2O predominantly plays a role in water and pear, a representative of fruits. Hydroid ions predominantly play a role in tomatoes and carrots, which are representative of fruits and vegetables. Potassium ions predominantly play a role in ginger and potatoes, which are representative of root vegetables.

Figure 11 illustrates a simple molecular behaviour model in the vacuole, estimated from measurements and simulated results. The polar molecule H_2O predominantly plays a role in water and pear, which is a representative of the fruits.

Hydroid and potassium ions predominantly play a role in tomatoes and carrots, which are representative of fruits and vegetables. Potassium ions predominantly play a role in ginger and potatoes, which are representative of root vegetables.

VI. CONCLUSIONS

The authors measured the reflective S-parameters S11 of six samples: pure water, pear, tomato, carrot, ginger, and potato, representing fruits, vegetables, and root vegetables, using a highly sensitive five-pin SMA probe. The higher sensitivity of the five-pin SMA probe compared to the open-end SMA probe was confirmed by measuring the five times conductance (G) values of water, NaCl, and KCl solutions. The measured data were plotted on a Smith chart, and equivalent circuits were synthesized using curve fitting. The plotted curves show two parts divided at a bending point. Since the low-frequency part is plotted along the impedance grid, its equivalent circuit is related to the cell wall. By grinding and 20-μm filtering, the cell wall was deleted, and the remaining part of the cell vacuole exhibits a specific circle feature at a high frequency above 2 GHz in the admittance curve measured from the reflective S-parameters. Using curve fitting on strict serial and parallel resonant frequencies when the susceptance (jB) equals zero, the precise equivalent circuits with elements of R_1, C_2, C_3, L_3, and R_3 were synthesized. The measured, simulated, and calculated element values, as well as the serial and parallel frequencies, were found to be in consistent agreement. Since the NaCl solution has electrical elements of polar H_2O and Na^+ and Cl^- ions, its equivalent circuit is the same as the cell vacuole, and its equivalent circuit elements were determined by curve fitting on the resonant frequencies. The NaCl solution can be used as an electrical reference for the cell vacuole's admittance. This research work, utilizing a highly sensitive SMA probe and curve fitting on the resonant frequencies, can be applied to the precise electrical analysis of both bio-material and chemical materials.

REFERENCES

[1] M. Festa, L. Lagostena, A. Carpaneto, "Using the plant vacuole as a biological system to investigate the functional properties of exogenous channels and transporters," *Biochimica et Biophysica Acta*, 1858, pp. 607-612,2016. DOI:10.1016/j.bbamem.2015.09.022
[2] A. Caeiro, J. Canhoto, P.R.F. Rocha, "Electrochemical impedance spectroscopy as a micropropagation monitoring tool for plants: A case study of tamarillo Solanum betaceum callus," *iScience*, vol. 28 (211807), pp. 1-9. 2025. DOI: 10.1016/j.isci.2025.111807.
[3] Li, Liu, Y. D.M, J. Qian, B. Di, G. Zhang, Z.H. Ren, "Electrical impedance spectroscopy (EIS) in plant roots research: a review," *Plant Methods*, vol. 17, no. 118, pp. 1-25, 2021. DOI: 10.1186/s13007-021-00817-3.
[4] I. Jocsa, G.Vegvari, E.Vozary, "Electrical impedance measurement on plants: a review with some insights to other fields," Theor. Exp. *Plant Physiol*, vol. 31, pp. 359-375, 2019. DOI: 10.1007/s40626-019-00152-y.
[5] M. Grossi, B. Ricco, "Electrical impedance spectroscopy (EIS) for biological analysis and food characterization: a review," *Journal of Sensors and Sensor Systems*, vol. 6, pp. 303-325, 2017. DOI: 10.5194/jsss-6-303-2017.
[6] M. Hussain, A. El-Keblawy, N. Akhtar, A. S Elwakil, "Electrical Impedance Spectroscopy in Plant Biology," *Sustainable Agriculture Reviews*, vol. 52, pp. 395-416, 2021. DOI: 10.1007/978-3-030-73245-5 12
[7] K. Kadan-Jamal, M. Sophocleous, A. Jogc, D. Desagani, O. Trog-Sussholz, J. Georgiou, A. Avni, Y. Shacham-Diamanda, "Electrical impedance spectroscopy of plant cells in aqueous buffer media over a wide frequency range of 4 Hz to 20 GHz," *MethodsX*, vol. 8, pp. 1-10, 2021. DOI: 10.1016/j.bios.2020.112485.
[8] M. V. Haeverbeke, B. D. Baets, B. D. Bernard, M. Stock, "Plant impedance spectroscopy: a review of modelling approaches and applications," *Plant Biophysics and Modeling. Front. Plant Sci.*, vol. 14, 2023. DOI: 10.3389/ fpls.2023.1187573.
[9] L.F. Lima, A.L. Vieira, H. Mukai, C.M.G. Andrade, P.R.G. Fernandes, "Electric impedance of aqueous KCl and NaCl solutions: Salt concentration dependence on components of the equivalent electric circuit," *Journal of Molecular Liquids*, vol. 241, pp. 530-539, 2017. DOI: 10.1016/j.molliq.2017.06.069.
[10] C.S. Widodo, H. Sela, D. R. Santosa, "The Effect of NaCl Concentration on the Ionic NaCl Solutions Electrical Impedance Value using Electrochemical Impedance Spectroscopy Methods," The 8th Annual Basic Science International Conference, *AIP Conf. Proc.*, 05003, pp. 1-6, 2021. DOI: 10.1063/1.5062753.
[11] J. Slay, R. Sotner, T. J. Freeborn, J. Jerabek, L. Polak, J. Petrzela, "Distinguishing Liquid Solutions With Alcohol Using Electrical Impedance Measurements: Preliminary Study for Food Safety Applications," *IEEE Sensors Journal*, vol. 23(22), pp. 26997-27007, 2023. DOI: 10.1109/JSEN. 2023.3315798.
[12] A. Leo, G. A. Monteduro, S. Rizzato, A. Milone, G. Maruccio, "Miniaturized Sensors for Detection of Ethanol in Water Based on Electrical Impedance Spectroscopy and Resonant Perturbation Method-A Comparative Study," *Sensor*, vol. 22, no. 7, pp. 2742, 2022. DOI: 10.3390/s22072742.
[13] K. Chinen, I. Kinjo, "Two-port Equivalent Circuit Deduced from S-parameter Measurements of NaCl Solutions," *IETE Journal of Research*. 877(3), pp. 1-9, 2022. DOI: 10.1080/03772063.2022.2081264
[14] K. Chinen, S. Nakamoto, I. Kinjo, "Alcohol Solutions Impedance and Equivalent Circuits," *International Journal of Electrical and Computer Engineering Research*, vol. 4, no. 2, pp. 1-7, 2024. DOI: 10.53375/ijecer.2024.397.
[15] K. Chinen, S. Nakamoto, I. Kinjo, "RF Analysis of Fruit and Vegetables using Equivalent Circuits Deduced from S-parameters," *International Journal of Electrical and Computer Engineering Research*, vol. 3, no. 2, pp. 18-24, 2023. DOI: 10.53375/ijecer.2023.342.
[16] K. Chinen, S. Nakamoto, I. Kinjo, "Relationship Between Impedance Transition Point and Cell Wall in Plant Tissue," *Quest Journals, Journal of Electronics and Communication Engineering Research*, vol. 10, no. 3, pp. 9-18, 2024.
[17] K. Chinen, S. Nakamoto, I. Kinjo, "Plant Cell Vacuolar Impedance and Equivalent Circuit," *IOSR Journal of Electronics and Communication Engineering (IOSR-JECE)*, vol. 19, no. 3, pp. 74-80, 2024. DOI: 10.9790/2834-1903011826.
[18] N5230A(VNA) https://www.keysight.com/us/en/product/N5230A/2port-pnal-series.html.
[19] Nanovna-saver https://nanovna.com/?page id=90
[20] QucsStudio https://nanovna.com/?page id=90
[21] AWR Design Environment Platform https://www.cadence.com/en US/home/tools/system-analysis/rf-microwave-design/awr-design-environment-platform.html.
[22] Standard tables of food composition in Japan https://www.mext.go.jp/en/policy/science technology/policy/title01/detail01/ sdetail01/sdetail01/1385122.htm.